Feedback control of Selective Laser Melting

J.-P. Kruth, P. Mercelis, J. Van Vaerenbergh, T. Craeghs
Katholieke Universiteit Leuven, Department of Mechanical Engineering, Division PMA, Belgium

ABSTRACT: Selective Laser Melting (SLM) is a powder bed based Rapid Manufacturing (RM) process in which parts are built by selective melting of layers of powders by means of a laser source. The main advantage of this technique is the possibility of making very complex and custom made pieces in a rather fast way. In this paper a feedback control system for Selective Laser Melting is presented. A feedback control system with a high-speed CMOS camera and a photodiode has been installed on the SLM-machine developed at K.U.Leuven-PMA. Both sensors were used independently to keep the melt pool area constant, especially in the case of scanning overhanging structures in which the melt pool would become very large. First motivation for the feedback system and the outline of the feedback system will be described. Next case studies are presented, in which both the photodiode as the CMOS camera have been used to control the SLM - process. Clearly, the feedback control system can improve the surface quality of the lower surface of the overhang.

1 Introduction

In the family of the powder bed based Rapid Manufacturing techniques, the direct full melting of powders in stead of using binder materials, has been studied at first on the end of the '90 (Meiners, 1999, Over et al., 2001). Until today, all existing additive manufacturing technologies (like SLS and SLM) use fixed process parameters during the scanning of individual vectors. With most processes, different parameter sets are defined, but each vector from the corresponding vector set is scanned with the set's fixed parameters (scanning speed, laser power, spot size, etc.). An example of different vector types and parameters is the distinction that is made between skin (at the outer surface of the layer) and core (at the inner of the layer) vectors and their corresponding parameters. Finding the appropriate process parameters for a certain powder material is most often done by labor intensive trial and error experiments, in order to define the feasible process window (Meiners, 1999).

Next to the small process windows, also the geometry of the part largely influences the process' stability. Many geometrical features, like sharp corners, down-facing surfaces, etc. cannot be accurately produced using fixed scanning parameters. The main reason for these bad results is the large variation in conductive heat transport caused by a change in local part geometry. Figure 1 demonstrates two problems: a bad part contour at sharp corners and dross formation at down-facing surfaces.

2 Equipment for SLM process monitoring

An in-process monitoring system based on a high speed CMOS camera and photodiode has been developed at K.U.Leuven (Mercelis, 2007). Figure 2 shows this prototype monitoring system mounted on

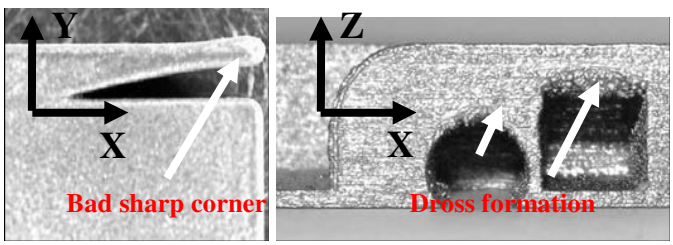

Figure 1: (left) top view of bad part contour at sharp corner (right) side view of dross formation at down facing surfaces

the own-built SLM machine of K.U.Leuven. Since the camera and photodiode look at the process through the beam deflection unit, the system can be used to observe the laser spot and melt pool at all times, regardless of the movement of the laser spot. The emitted radiation from the melt pool depends on the melt pool temperature according to Planck's law.

Initial tests using the system indicated that the CMOS camera and the photodiode both can extract useful information from the melt pool radiation (see Figure 3). While the photodiode integrates all melt pool radiation, the CMOS camera offers a 2D image, from which the melt pool geometry can be extracted.

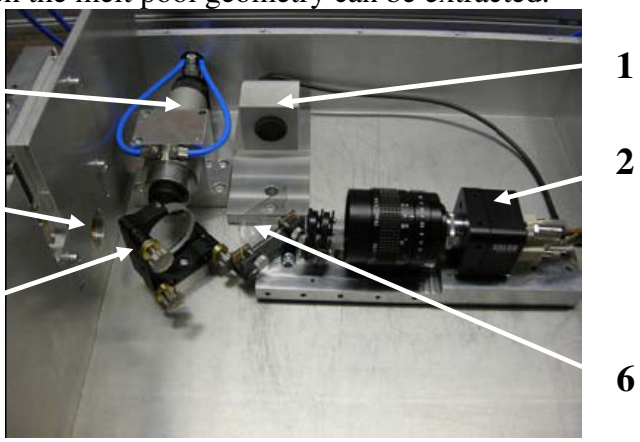

1 Photodiode
2 CMOS camera
3 Fibre laser output
4 Scanner
5 45° mirror
6 45° mirror

Figure 2: prototype monitoring system

3 Melt pool observation during SLM

3.1 Determination of the melt isotherm

In order to recognize the melt pool, the color level corresponding with the melt isotherm must be identified. An analytical calculation of this melt color level is impossible because of different reasons (Mercelis, 2007). However, it is possible to extract the melt color level from the recorded images experimentally. Figure 4 demonstrates the image of one scan track of molten powder on a base plate, taken by a light microscope. The width of this track is 677 µm. A micrometer to pixel calibration scale is then created.

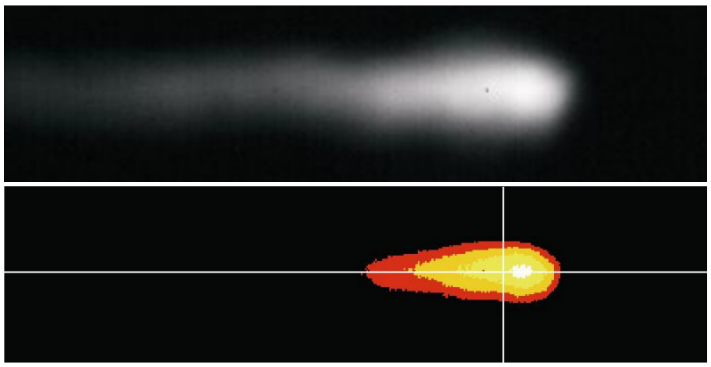

Figure 3 Typical image of SLM melt pool, (top) raw and (bottom) after image post-processing

Figure 5 shows the cross section of melt pool image, across the dotted line indicated (Figure 5, left). The color level at which the distance between the ascending and the descending limb of the cross section is approximately equal to 677µm, is the melt color level. This level has been determined at 15. Thus, it is assumed that a pixel color level of 15 or higher represents molten material.

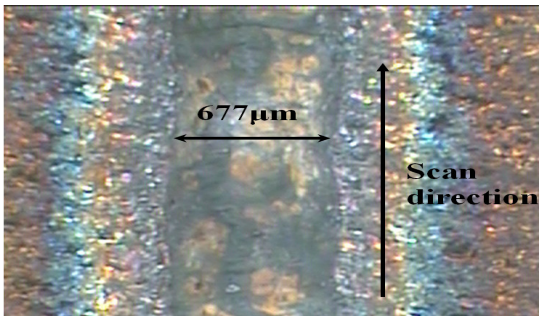

Figure 4 Measurement of one scan track to determine the threshold value

This assumption is only valid if exactly the same test settings are used as in this experiment.

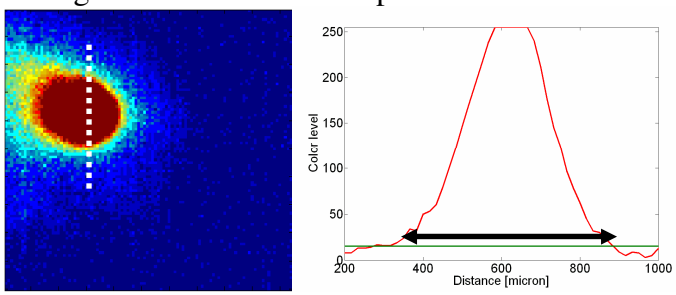

Figure 5 Cross section of melt pool image to determine the threshold value (for stainless steel powder)

3.2 Calculation of melt pool geometry

The geometry calculation algorithm uses the melt temperature level to extract the area, length and width of the melt pool. Most often, scan tracks are parallel with the X or Y direction of the scanner. Therefore, the melt pool will be oriented horizontally or vertically. Only in case of contour scanning, the melt pool orientation is undefined. Therefore, the calculated length and width values are only meaningful for X or Y oriented scans. The calculated melt pool area, on the other hand, is valid regardless of the scan orientation, since the algorithm counts the number of pixels above the melt temperature level, and multiplies it with a geometric factor.

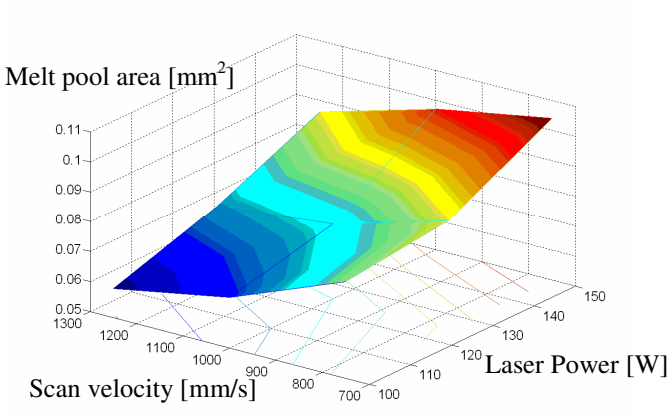

Figure 6 Melt pool area versus scanning velocity and laser power for stainless steel powder

3.3 Steady - state melt pool observation

Several researchers developed theoretical models about the influence of laser power and scan speed on the melt pool area (Romer, 1999, Mercelis, 2007). These models predicted an almost linear rise of the melt pool area with laser power and an exponentially decaying influence of the source velocity on the melt pool area. At low scan velocities, the melt pool raises for a higher scanning velocity. The melt pool size becomes maximal for a certain scanning velocity and afterwards the trend becomes decaying, as expected intuitively and as predicted by theory. Figure 6 demonstrates the melt pool area for 3 different laser powers (100, 125, 150W) and 3 three different scan velocities (750, 1000, 1250 mm/s). It is clear from the picture that these scan speeds are in the "decaying zone". The expected trend can be clearly observed: for higher laser power and for lower scan speed, the steady - state melt pool area is higher.

3.4 Transient melt pool response

For the SLM process in general about 50 process-parameters can be found (Van Elsen, 2007). A simple analytical model for SLM predicts an approximately

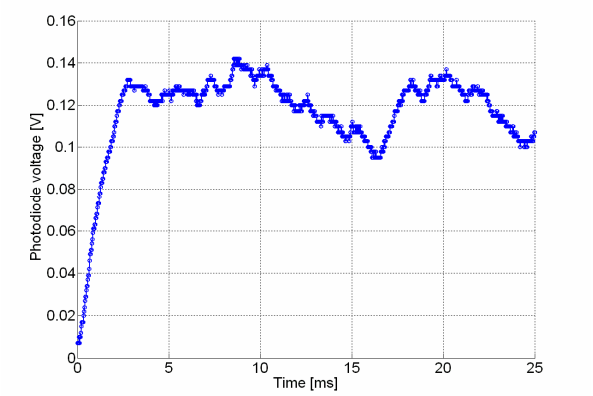

Figure 7 Transient response of the photodiode voltage with laser power 100 W and scan speed 300 mm/s.

first order transient behavior for the melt pool temperatures with the laser power as input variable. The SLM process can then be seen as a SISO system with transfer function $G(s)$ between melt pool area S and laser lower P is then

$$G(s) = \frac{K}{1+\tau s}$$

with K the steady-state coefficient and τ the time constant (by definition the time needed to reach 63% of the steady state value).

Figure 7 shows the transient response of the photodiode voltage (which is proportional to the melt pool area) while observing one scan track of one layer of powder on a base plate with P = 100 W and v = 300 mm/s. The time constant τ in this case is equal to about 1.5 ms.

3.5 Observation of local overheating at overhanging planes

For three dimensional parts, the border conditions of the conductive heat transport have a very large influence on the melt pool dimensions. At solid-supported zones, the conductive heat transport will be large, of course depending on the bulk material's conductivity. However, at powder-supported zones, like e.g. during scanning of an overhanging plane, the heat conduction rate may be more than 100 times smaller than the corresponding bulk conductivity (Rombouts, 2006, Carslaw & Jaeger, 1990, Carson et al., 2005). Knowing that in general in SLM fixed process parameters determined experimentally for solid-supported geometries are used, one can imagine that the heat input is far too large when a powder-supported zone is scanned. This result in a much too large melt pool, which sinks into the supporting powder due to gravity and capillary forces. This leads to a bad surface quality of the overhang plane.

Figure 8 shows two ways of scanning for a horizontal overhanging plane. These two scanning directions will be referred to as parallel scanning (i.e. transition line solid/powder of the overhang is parallel to the scanning direction) or perpendicular scanning (i.e transition line solid/powder is perpendicular to the scanning direction). Three zones are indicated: A and C are solid supported zones, while B is a powder supported zone.

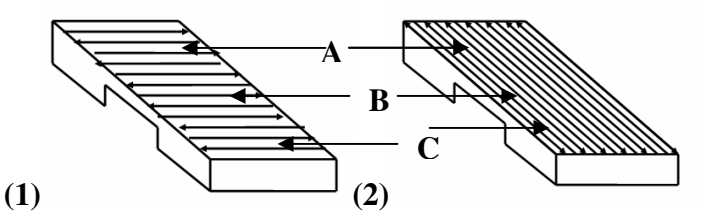

Figure 8 Two possible ways of scanning an overhanging structure (1) parallel scanning (2) perpendicular scanning

Figure 9 shows the melt pool areas during parallel scanning and perpendicular scanning of a horizontal overhang. For both the parallel and the perpendicular scanning melt pool area signals, the three different zones are indicated. In the zones A and C, the melt pool area stays close to a certain value, with only little fluctuations due to noise in the signal. In the B zone the area grows much larger. With the parallel scanning the melt pool area is also larger when reaching the end of the overhang.

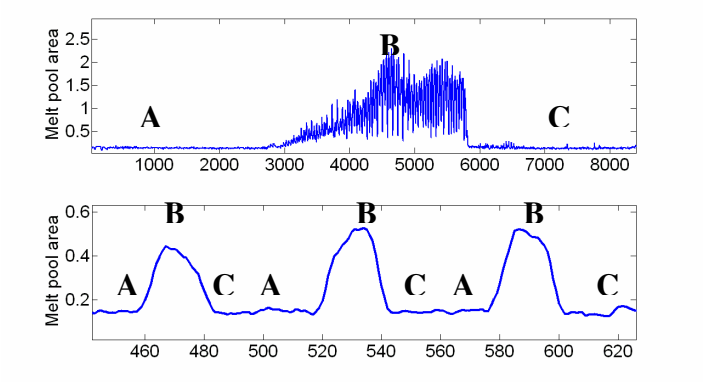

Figure 9 Melt pool area during parallel scanning (top) and perpendicular scanning of an overhang. The horizontal axes represents the number of samples, with sampling frequency = 1207 Hz.

4 Local process control of SLM: controller setup

Feedback control has been implemented using the coaxial optical monitoring system shown above (Figure 2). Two different feedback signals were used: first by the photodiode, second by the high speed CMOS camera. It has been proved that the photodiode signal is proportional to the melt pool area (Mercelis, 2007).

In order to stabilize the melt pool behavior (melt pool area) during the process, the laser power that is applied to the powder material is controlled in real-time, during scanning. Since the control of the laser power level is independent of the laser spot motion, the laser power can be adjusted even during the scanning of a single vector.

Figure 10 shows a schematic overview of the feedback loop. In this scheme e and ΔP respectively represent the error and the PID controller output with:

$$e = PV_{ref} - PV$$

$$\Delta P = u(t) = K_c(e + \frac{1}{T_i}\int_0^t edt + T_d\frac{de}{dt})$$

The process variable (PV) is the variable that will be measured during the scanning. In case of using the photodiode the process variable is the photodiode voltage, in case of using the CMOS camera the process variable is the number of pixels that have a higher color level than the threshold value. In both cases, PV is a measure of the melt pool area.

The desired setpoint value for both sensors is function of the chosen parameters (laser power, scan speed, layer thickness …) and need to be determined experimentally for every different parameter set used.

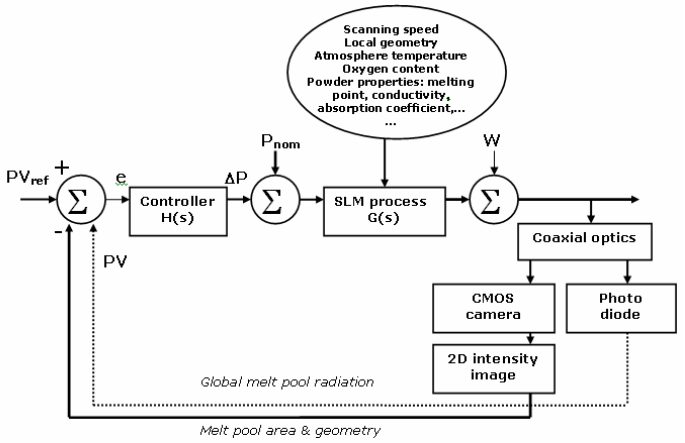

Figure 10 Schematic overview of feedback loop

5 Control of overhang geometries

The performance of the feedback control system, based on the photodiode as well as on the CMOS camera has been evaluated. For both the scanning of the first layer of an horizontal overhang, as well as the scanning of a tower with several types of overhangs, the performance of the photodiode as well the CMOS camera-based control loop will be discussed.

5.1 First layer of horizontal overhang

Table 1 (see annex) gives an overview of the parallel scanning and perpendicular scanning of square overhanging geometries, first with the photodiode and second with the CMOS camera based feedback control loop. Also the resultant pieces are shown.

The experiment with the photodiode control was performed with titanium powder, with P = 80 W, v = 80 mm/s, layer thickness 80 µm. The pressure in the

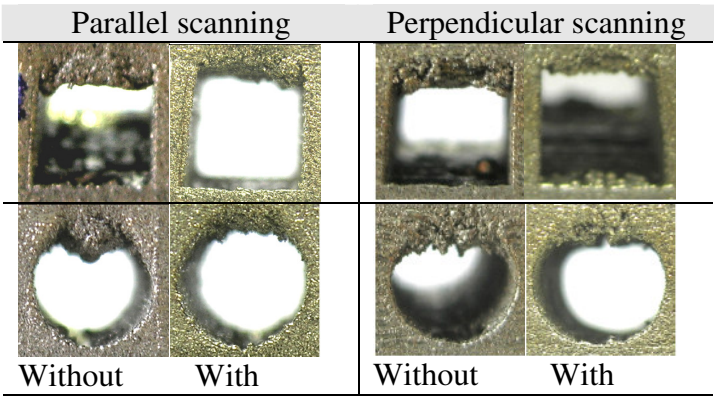

Figure 13 Comparison of tower with overhanging structure (left) without and (right) with feedback
Photodiode based, vacuum

process chamber was near to vacuum. The experiment with the CMOS camera based control was performed with stainless steel powder, with P = 100 W, v = 300 mm/s and layer thickness 30 µm. In this case, the pressure in the chamber was atmospheric pressure.

In the experiment with the photodiode control loop, comparison between the parts produced with and without feedback control demonstrates that the surface of the overhang geometry is clearly improved with feedback control. In the experiment with the CMOS camera based control loop, also the quality of the first layer is improved. Attention has to be paid that the first layer of the overhang doesn't become too thin. In other experiments a very high scan speed has been used, which leads to an incomplete first layer (Figure 11). This can be dangerous because the incomplete layer can break when scanning the next layers, and lead to failure of the whole piece and eventually damage of the coater.

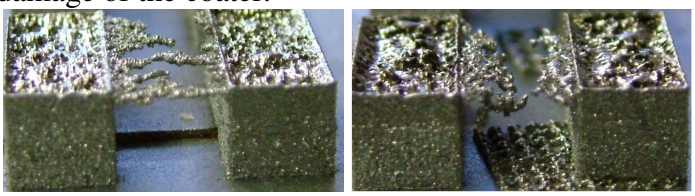

Figure 11 Failure of the first of layer of overhanging structure, scanned with feedback control of laser power and high scan velocity, (left) perpendicular scanning; (right) parallel scanning

For a fixed laser power the depth of the melt pool is less with higher scan velocity. Because the controller lowered the used laser power at the overhang layer, the first layer at the overhang geometry became incomplete.

However, for both the photodiode and the CMOS camera based control loop, the melt pool area signals show that the controller is able to keep the melt pool area close to the setpoint value.

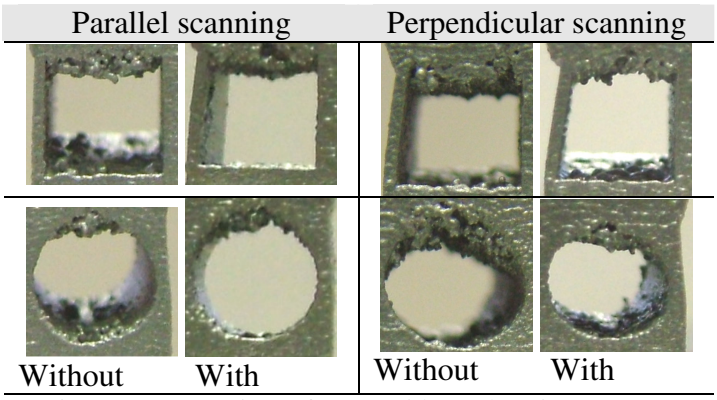

Figure 12 Comparison of tower with overhanging structure (left) without and (right) with feedback
CMOS camera based, atmospheric pressure

5.2 *Tower with overhanging structures*

In order to evaluate the current real-life performance of the feedback system, a benchmark part was designed, including a number of different overhang geometries. The benchmark part included straight and circular overhang geometries with a length, respectively diameter of 2, 5 and 8 mm, in X as well as in Y direction. Only the overhang geometries of 5 mm will be shown. This benchmark part was built four times with stainless steel powder; (1) using fixed scanning parameters in vacuum, (2) using fixed scanning parameters in atmospheric pressure, (3) using feedback control of the laser power based on the photodiode in vacuum and (4) based on the CMOS camera in atmospheric pressure. Figure 13 demonstrates the comparison between overhanging structures of tower 1 (fixed parameters, vacuum) and tower 2 (photodiode based, vacuum).

For the circular geometries, it can be seen from Figure 13 that the best improvement is achieved in case of parallel scanning. This is a logical result, since perpendicular scanning involves much faster variations in the melt pool volume, that cannot be counteracted as efficiently as the slower variations in case of parallel scanning. For the square geometries, there is no clear difference between the performance of parallel and perpendicular scanning. This results from the fact that in case of perpendicular scanning, there is enough time to adjust the laser power, due to the length of the overhang vectors. This is in contrast with circular overhangs, where the controller needs to react each time a vector approaches the overhang zone, thus much less time is available to counteract.

Figure 12 demonstrates the comparison between overhanging structures of tower 3 (fixed parameters, atmospheric pressure) and tower 4 (CMOS camera

based, atmospheric pressure). Even in atmospheric pressure, there is an improvement with generally the same conclusions as in vacuum, but less significant. When the overhang geometries with fixed parameters are compared between vacuum and atmospheric pressure, there is a clear improvement with scanning in atmospheric pressure. This is because in vacuum the melt evaporates more easily, and the recoil pressure on the melt pool makes the melt pool sink into the loose powder on the overhang (Kruth et al., 2003).

6 Conclusion

In the world of the Rapid Prototyping and Rapid Manufacturing processes, feedback (and eventually feedforward) control of the process opens new possibilities in the control of the quality of the products. This paper presented a monitoring and control system for Selective Laser Melting. The proposed system uses a photodiode, of which the signal reflects a measure of the melt pool area, and a high speed CMOS-camera, which provides an image of the melt pool area itself. Both the photodiode as the CMOS-camera can be integrated in a feedback control system.

In general it can be concluded that both the photodiode as the CMOS camera based control system proved to work; the melt pool area with scanning of overhanging structures can be controlled. However still some improvement is possible. When using the CMOS camera based control loop, other process variables than the melt pool area can be used, e.g. melt pool length, or melt pool length/ width ratio.

The used controllers this far have also limited bandwidth. This means that at high scan velocities the controller only justifies the laser power after a relatively large distance. Thus, when scanning very small overhanging structures, there will be only very little improvement.

A first important step in the control of the SLM process has been made. In the future model based controllers with high bandwidth will be developed for further improvement of the control of the process.

7 References

Carslaw, H.S. & Jaeger, J.C., 1990, *Conduction of heat in solids.* Oxford University Press

Carson, J.K., Lovatt, S.J., Tanner, D.J. & Cleland, A.C., 2005, Thermal conductivity bounds for isotropic, porous materials. *Int. Journal of Heat and Mass Transfer*, 48:2150-2158.

Kruth, J.-P., Froyen, L., Van Vaerenbergh, J., Mercelis, P., Rombouts, M., Lauwers, B., 2003, Selective Laser Melting of Iron Based Powders. *Journal of Material Processing Technology, 149, 616-622*

Meiners, W., 1999, *Direktes Selektives Laser Sintern einkomponentiger metallischer Werkstoffe*. PhD thesis, Aachen

Mercelis, P., 2007, *Control of Selective Laser Melting*, PhD thesis, Katholieke Universiteit Leuven

Over, W. Meiners, W., Wissenbach, K., Lindemann, M. & Hamman G., 2001, Selective Laser Melting: a new approach for the direct manufacturing of metal parts and tools. In *Proceedings of the Laser Assisted Net Shape Engineering (LANE) Conference, 3,* 391-398

Rombouts, M., 2007, *Selective Laser Sintering/Melting of iron based powders,* PhD thesis, Katholieke Universiteit Leuven007

Romer G., *Modelling and control of laser surface treatments.* PhD thesis, University of Twente, 1999.

Van Elsen, M., 2007, *Selective Laser Melting: a new optimisation approach*, PhD thesis, Katholieke Universiteit Leuven.

	Photodiode loop 130 W, 80 mm/s, vacuum	CMOS Camera loop 100 W, 300 mm/s, atmospheric pressure
Parallel scanning	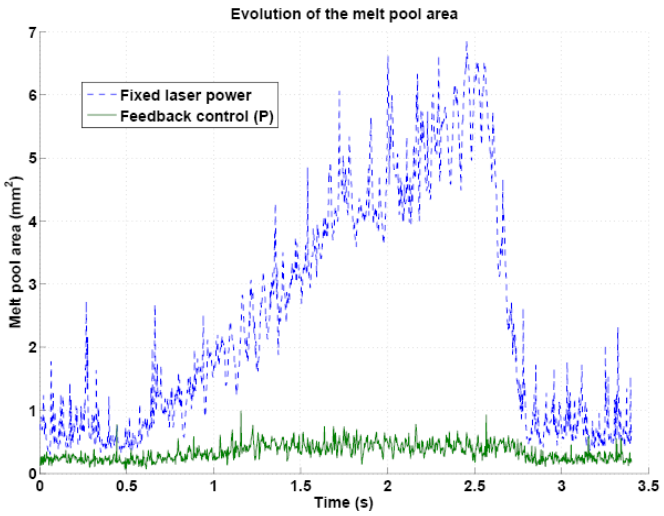 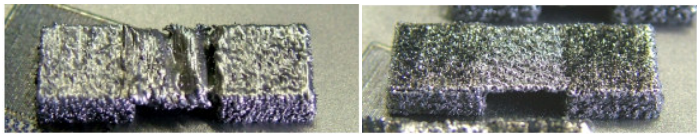 Fixed laser power Feedback control	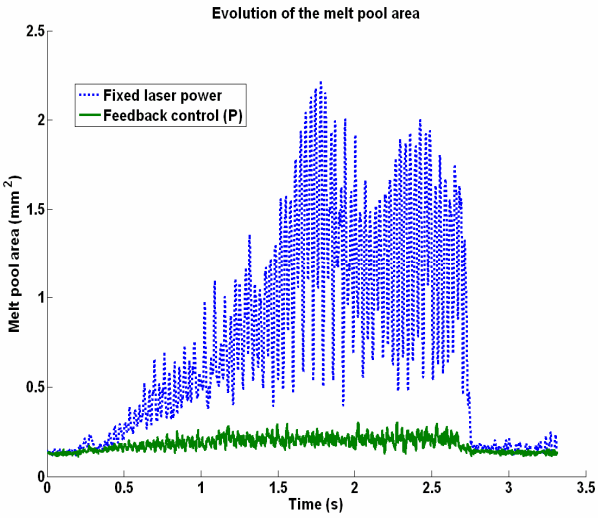 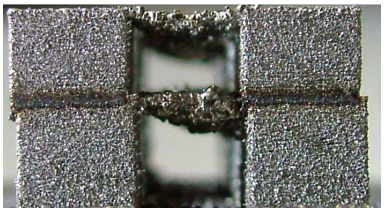 Bottom: fixed laser power Top: feedback control of laser power
Perpendicular scanning	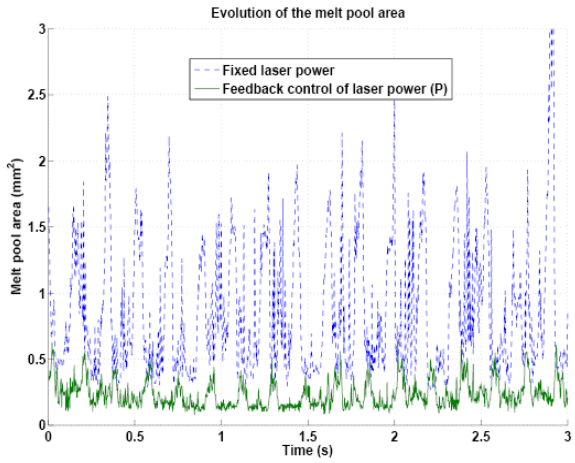 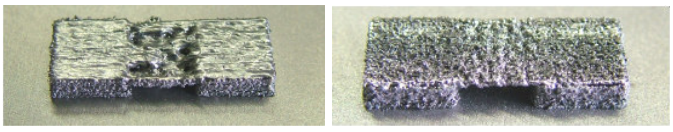 Fixed laser power Feedback control	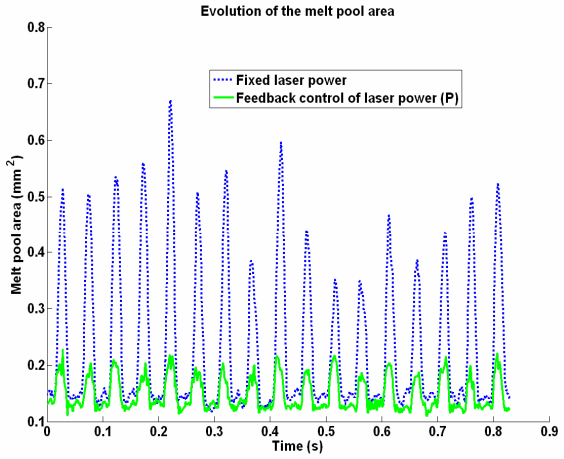 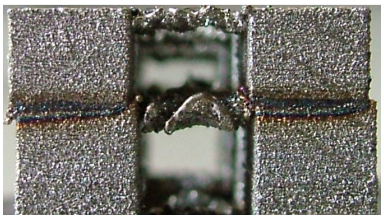 Bottom: fixed laser power Top: feedback control of laser power

Table 1: overview of parallel scanning and perpendicular scanning square overhanging geometries with photodiode (titanium powder, in vacuum) and CMOS camera based (stainless steel, atmospheric pressure) feedback control loop